Tomohiro Tachi[1]
Department of General Systems Studies,
Graduate School of Arts and Sciences,
The University of Tokyo,
Tokyo 153-8902, Japan
e-mail: tachi@idea.c.u-tokyo.ac.jp

Thomas C. Hull
Department of Mathematics,
College of Arts and Sciences,
Western New England University,
Springfield, MA 01119
e-mail: thull@wne.edu

Self-Foldability of Rigid Origami

When actuating a rigid origami mechanism by applying moments at the crease lines, we often confront the bifurcation problem where it is not possible to predict the way the model will fold when it is in a flat state. In this paper, we develop a mathematical model of self-folding and propose the concept of self-foldability of rigid origami when a set of moments, which we call a driving force, are applied. In particular, we desire to design a driving force such that a given crease pattern can uniquely self-fold to a desired mode without getting caught in a bifurcation. We provide necessary conditions for self-foldability that serve as tools to analyze and design self-foldable crease patterns. Using these tools, we analyze the unique self-foldability of several fundamental patterns and demonstrate the usefulness of the proposed model for mechanical design.
[DOI: 10.1115/1.4035558]

1 Introduction

In mechanical designs based on rigid origami, the folding motion is often achieved by rotational actuators that apply bending moments at each foldline between facets. This self-folding principle is very powerful in different applications; it can be used to design reprogrammable matter [1], self-folding machines [2], or to obtain 3D microstructures based on printing patterns [3]. When using self-folding techniques, we always encounter a common question: Is a given configuration possible to be realized by a set of actuators? If so, how? Indeed, the rigid foldability condition [4,5] is a necessary condition for a rigid origami to be actuated as a mechanism; however, this is not at all sufficient. For example, consider a vertex composed of three mountains and three valleys. This can be actuated into two clearly distinct configurations even though they follow the same MV assignment (Fig. 1). Once the vertex starts to pop up or pop down, it cannot flip to the other side without unfolding everything. This bifurcating nature and multistability of origami vertices is an interesting phenomena attracting the attention of scientists [6–8]. However, from the viewpoint of mechanical design, we often want to avoid such bifurcations. The objective of this paper is to predict the way the model folds from the flat unfolded state and to enable a design of motion via the computation an appropriate set of applied moments. The example of Fig. 1 tells us that we need extra care in order to achieve such a goal. This is not a straightforward problem, as we can observe that even with a set of proper mountain valley folding moments, we may easily encounter bifurcations at the flat state. This flat state singularity is the very reason that the folding of rigid foldable origami such as the Miura-ori or the Resch pattern is difficult at the beginning but is easy when correctly folded for a finite amount.

In this paper, we will pose the mathematical problem of *self-folding*: To know if there exists a set of moments applied on each hinge, which we later call a driving force, to enable a desired folding motion of a given crease pattern. We give basic theoretical tools for self-folding with which we can analyze and design rigid origami mechanisms based on self-folding.

We also consider a subproblem of self-foldability: Self-foldability with rotational spring driving forces that we define rigorously later in this paper. In this situation, we have a physical implementation of actuators where each edge has a prescribed target fold angle and independently tries to get closer to the target fold angle when actuated, as if torsion springs are attached to creases. We define a mathematical model of such a system and call it a rotational spring driving force. Rotational spring driving forces can model actual methods used in self-folding contexts, e.g., multilayered shape memory materials [1,2] or polymer gel [8]. If a rigid origami is self-foldable with a rotational spring driving force, this can be a very robust system, programmable without active sensing or instantaneous feed-back control.

In this paper, we concentrate on the problem of finding a rotational spring driving force that uniquely self-folds from and to desired rigid origami states. Is this always possible? If not, can we characterize uniquely self-foldable patterns? We believe that the general problem leads to interesting open problems in mathematics and theoretical computer science. As evidence, we will investigate the self-foldability of some interesting examples that can be helpful to grasp the essence of the self-folding problem.

2 The Self-Folding Problem

Self-foldability is the problem of asking if a rigid folding path from a flat unfolded state to a 3D-folded state can be actuated using a set of driving force (rotational moment) functions without causing a bifurcation at any state. Here, we ignore the inertial effects; in such a system, the springs and dampers dominate, and thus, we can assume that we instantaneously obtain a critical (angular) velocity proportional to the (moment of) force. Self-foldability is an especially important problem at the flat unfolded state where rigid origami constraints degenerate.

DEFINITION 1 (Configuration Space). *For a rigid origami with n creases (edges), a configuration is the set of fold angles $\rho_1,\ldots,\rho_n$ of creases 1,…, n of the crease pattern; this can be represented as a point $\boldsymbol{\rho} = [\rho_1,\ldots,\rho_n]^{\mathsf{T}}$ in n-dimensional parameter space, where n is the number of creases. A rigid folding, i.e., valid configuration, is a configuration which satisfies a set of constraints derived from isometries (Eq. (1) below) and nonintersection of the facets. The set of rigid foldings from the same rigid origami is a subset of the parameter space and is called the configuration space.*

DEFINITION 2 (Continuous Folding). *A well-behaved continuous rigid folding $\boldsymbol{\rho}(s)$ from a rigid folding $\boldsymbol{\rho}(0)$ to $\boldsymbol{\rho}(s_{\text{target}})$ is an arc length-parameterized piecewise C^1 curve in a valid configuration space in n-dimensional parameter space. Because it is piecewise C^1, there are at most two tangent vectors $\mathbf{v}_+(s_0) :=$*

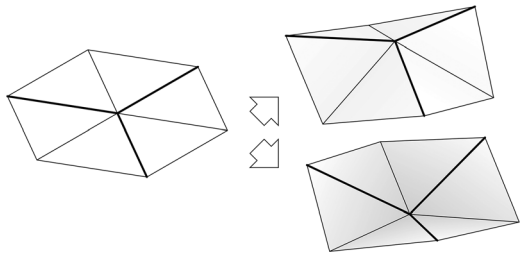

Fig. 1 A vertex with three mountains and three valleys. This can pop up or pop down even with the same MV assignment. Note that pop-up state has sharper mountains and pop-down state has shaper valleys.

[1]Corresponding author.

Manuscript received October 11, 2016; final manuscript received December 10, 2016; published online March 9, 2017. Assoc. Editor: James Schmiedeler.

$\lim_{s\to s_0+}(d\boldsymbol{\rho}(s)/ds)$ *and* $\mathbf{v}_-(s_0) := \lim_{s\to s_0-}(d\boldsymbol{\rho}(s)/ds)$ *at a valid configuration*.

Consider a set of well-behaved continuous foldings passing through a configuration. The set of tangent vectors of such foldings at the configuration form a region when projected on the unit sphere, which we call valid tangents.

We believe that "well-behaved folding" defined as a piecewise smooth curve captures any process of an actual folding motion that has only a finite number of singular positions. At singular positions, especially at the origin (the flat, unfolded state), the two velocity vectors defined capture the irreversible nature of self-folding and self-unfolding, i.e., self-unfolding is usually easier than self-folding. Figure 2 illustrates the above definitions. Valid tangents may form a nonconnected region on the unit sphere, and the self-foldability problem is deeply related to the geometry of valid tangents.

DEFINITION 3 (Driving Force). *A driving force is a continuous vector field in the parameter space:* $\mathbf{f}(\boldsymbol{\rho}) = [f_1(\boldsymbol{\rho}), \ldots, f_n(\boldsymbol{\rho})]^{\mathrm{T}}$. *A driving force is conservative if it is the negative gradient of some* C^1 *scalar field* $U(\boldsymbol{\rho})$, *i.e.,* $\mathbf{f}(\boldsymbol{\rho}) := -\nabla U(\boldsymbol{\rho})$. *We call* $U(\boldsymbol{\rho})$ *the potential energy*.

Also, we call a conservative driving force and potential energy a rotational spring driving force and rotational spring potential energy, respectively, if the potential energy is an additively separable function, i.e., the function can be represented as the sum of functions of each fold angle: $U(\boldsymbol{\rho}) = U_1(\rho_1) + \cdots + U_n(\rho_n)$.

In physical sense, a driving force represents a set of moments applied to the hinges. We call it a "force" in the generalized sense, as an energy gradient in some coordinate system. As already mentioned, rotational spring driving forces yield more robust and easy-to-implement systems of self-folding than general potential energy or nonconservative forces that require instantaneous feedback control.

DEFINITION 4 (Constrained Force). We define the constrained forces along a well-behaved continuous rigid folding $\boldsymbol{\rho}(s)$ to be $f_+(s) := \mathbf{v}_+(s) \cdot \mathbf{f}(\boldsymbol{\rho}(s))$ and $f_-(s) := \mathbf{v}_-(s) \cdot \mathbf{f}(\boldsymbol{\rho}(s))$. We call the former the forward force and the latter the backward force. If a driving force is conservative, then, $f_+(s_0) = -\lim_{s\to s_0+}(\partial U/\partial \boldsymbol{\rho}) \cdot (d\boldsymbol{\rho}/ds) = -\lim_{s\to s_0} +(dU(\boldsymbol{\rho}(s))/ds)$.

DEFINITION 5 (Self-Foldable). A well-behaved continuous folding $\boldsymbol{\rho}(s)$ from a rigid folding $\boldsymbol{\rho}(0)$ to $\boldsymbol{\rho}(s_{\text{target}})$ is self-foldable by driving force $\mathbf{f}(\boldsymbol{\rho})$ if at any point $\boldsymbol{\rho}(s)$ for $s \in [0, s_{\text{target}})$, the forward force $f_+(s)$ is positive and takes a local maximum among the valid tangents at s. Here, we can observe the continuity of vector directions by calculating an intersection of the configuration space with a sphere of radius ϵ around the point when $\varepsilon \to 0$. We call a well-behaved continuous folding $\boldsymbol{\rho}(s)$ uniquely self-foldable if $\boldsymbol{\rho}(s)$ is the only well-behaved continuous folding, that is, self-foldable by $\mathbf{f}$.

3 Basic Kinematics and the Singularity Issue at the Flat State

A rigid folding is valid if and only if it is piecewise isometric and does not self-intersect. If the origami paper forms a disk, the isometry constraints of a rigid origami can be represented by the identity of a rotational matrix product [9,10] as follows: For each interior vertex with foldline direction vectors represented by $\boldsymbol{\ell}_i = [\ell_i^x, \ell_i^y, 0]^\top$ for $i = 0, 1, \ldots, n-1 \pmod n$, their fold angles ρ_i must satisfy

$$\vec{R} = \vec{I}, \text{where } \vec{R} := \vec{R}(\boldsymbol{\ell}_0, \rho_0)\vec{R}(\boldsymbol{\ell}_1, \rho_1)\cdots\vec{R}(\boldsymbol{\ell}_{n-1}, \rho_{n-1}) \tag{1}$$

and $\mathbf{R}(\boldsymbol{\ell}_i, \rho_i)$ is an orthogonal matrix representing the rotation by angle ρ_i about an axis along $\boldsymbol{\ell}_i$ passing through the origin. As Eq. (1) is a set of polynomial equations of cosines and sines of the fold angles on a compact domain ($-\pi \le \rho_i \le \pi$ for all i), the valid set of variables is a closed set. We also define the nonintersection condition to allow the paper to touch (but not penetrate) itself. This implies that the configuration space of an origami disk is a closed set.

Consider a configuration where each crease is folded from the original direction $\boldsymbol{\ell}_i$ to a 3D direction $\mathbf{L}_i = [L_i^x, L_i^y, L_i^z]^\top$. The partial derivative of the left-hand side of Eq. (1) is calculated as [11]

$$\frac{\partial \mathbf{R}}{\partial \rho_i} = [\mathbf{L}_{i\times}] \tag{2}$$

where $[\mathbf{L}_{i\times}]$ is the matrix representing the cross product operation

$$[\mathbf{L}_{i\times}] := \begin{bmatrix} 0 & -L_i^z & L_i^y \\ L_i^z & 0 & -L_i^x \\ -L_i^y & L_i^x & 0 \end{bmatrix}$$

Therefore, the first-order motion satisfies

$$\sum_{i=0,\ldots,n-1} \dot{\rho}_i \mathbf{L}_i = \mathbf{0} \tag{3}$$

This gives three equations for each interior vertex of a crease pattern. The configuration space is tangent to at least a $e_{\text{in}} - 3v_{\text{in}}$-dimensional linear space for an origami model with e_{in} creases and v_{in} interior vertices. However, in the flat unfolded state of $\mathbf{L} = \boldsymbol{\ell}$, the third row of Eq. (3) degenerates, giving us a higher-dimensional tangent space with at least $e_{\text{in}} - 2v_{\text{in}}$ dimensions. The flat state forms a connecting point of otherwise separated configuration space components.

4 Degree-4 Flat-Foldable Single Vertex

Consider a degree-4, flat-foldable single vertex with sector angles $\alpha, \beta, \pi-\alpha, \pi-\beta$ (Fig. 3). Its fold angles ρ_0, ρ_1, ρ_2, ρ_3 form a four-dimensional parameter space, and the relationships between these angles give us a valid configuration space that is the union

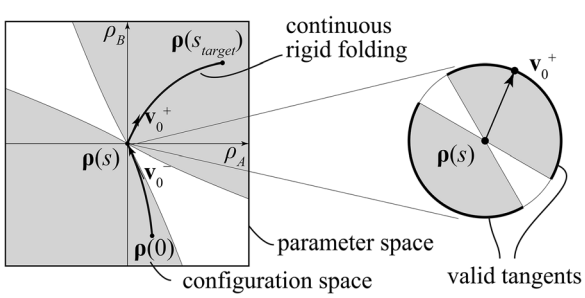

Fig. 2 Tangent vectors of well-behaved continuous rigid folding and valid tangents

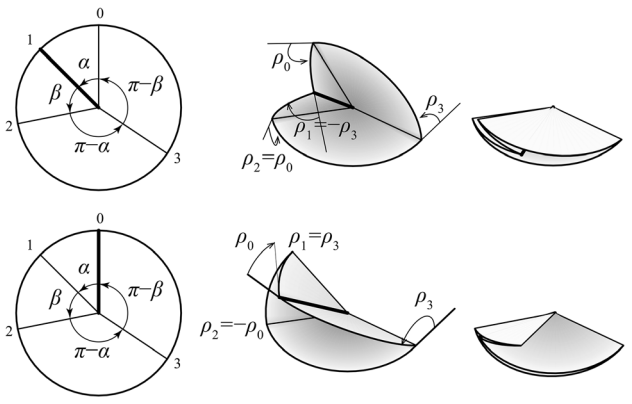

Fig. 3 Two folding modes of a flat-foldable vertex with four creases. The fold angles of opposite creases have the same magnitude.

of the following two modes [12] (see the Appendix for details, Fig. 3)

$$\mathbf{t} = \left[\tan\frac{\rho_0}{2}, \tan\frac{\rho_1}{2}, \tan\frac{\rho_2}{2}, \tan\frac{\rho_3}{2}\right]^\top = \begin{cases} [t, -pt, t, pt]^\top & \text{mode 1} \\ [qt, t, -qt, t]^\top & \text{mode 2} \end{cases} \tag{4}$$

where p and q are the constants given by

$$p = p(\alpha, \beta) = \frac{1 - \tan\frac{\alpha}{2}\tan\frac{\beta}{2}}{1 + \tan\frac{\alpha}{2}\tan\frac{\beta}{2}} \tag{5}$$

$$q = q(\alpha, \beta) = \frac{\tan\frac{\alpha}{2} - \tan\frac{\beta}{2}}{\tan\frac{\alpha}{2} + \tan\frac{\beta}{2}} \tag{6}$$

Notice that $0 < |p| < 1$ and $0 < |q| < 1$. The folding modes 1 and 2 are each 1-manifolds embedded in four-dimensional parameter space that intersect only at $\mathbf{t} = \mathbf{0}$ (Fig. 4). We, respectively, call them configuration curves 1 and 2. Note that at $\mathbf{t} = \mathbf{0}$, the valid tangents lie within the two-dimensional space defined by Eq. (3).

THEOREM 1. *For any rigidly foldable, flat-foldable degree-4 vertex with an arbitrary starting and target configurations, there exists a rotational spring driving force that makes the vertex uniquely self-foldable.*

Proof. Let $\boldsymbol{\rho} = [\rho_0, \rho_1, \rho_2, \rho_3]^\top$ represent the configuration of the model. Assume by symmetry that the target $\boldsymbol{\rho}_T$ lies on configuration curve 1

$$\boldsymbol{\rho}_T = [\tau_0, \tau_1, \tau_2, \tau_3]^\top = [\tau_0, -\tau_3, \tau_0, \tau_3]^\top$$

We call the subsets of curve 1 separated by $\boldsymbol{\rho} = \mathbf{0}$ manifolds 1+ and 1−, such that curve 1+ includes $\boldsymbol{\rho}_T$.

We now claim that if there exists a potential energy function $U(\boldsymbol{\rho})$ with the conditions that

(1) U monotonically decreases along mode 1 toward the target state.
(2) U monotonically decreases along mode 2 toward the flat state.

then, $U(\boldsymbol{\rho})$ uniquely self-folds from any state to the target state along the shortest path from the initial and targets shapes.

The proof is as follows. Assume that above conditions are satisfied. If we start from a point on curve 1+, then a continuous rigid folding along the shortest path to target position $\boldsymbol{\rho}_T$ always has positive forward force $f_+(s) > 0$ because of condition 1. Therefore, this path is uniquely self-foldable by U.

Consider that the initial point is on curve 2. Then, a continuous rigid folding along the shortest path from any point $\boldsymbol{\rho} \neq \mathbf{0}$ on curve 2 to $\boldsymbol{\rho} \neq \mathbf{0}$ is uniquely self-foldable by U because of condition 2. Similarly, if we start from a point on curve 1−, the shortest path to $\mathbf{0}$ is uniquely self-foldable by U because of condition 1.

Once we arrive at $\boldsymbol{\rho} = \mathbf{0}$ there are four possible paths on which to travel. Here, the one along curve 1+ is uniquely chosen as the tangent vector $\mathbf{v}_+$ because

(1) The tangent direction toward 1+ is strictly energy decreasing as $f_+(s) > 0$ because of condition 1.
(2) The tangent direction toward 1− is strictly energy increasing as $f_+(s) < 0$ because of condition 1.
(3) The tangent direction along curve 2 in either direction is energy increasing since $f_+(s) < 0$ once we move away from $\boldsymbol{\rho} = \mathbf{0}$.

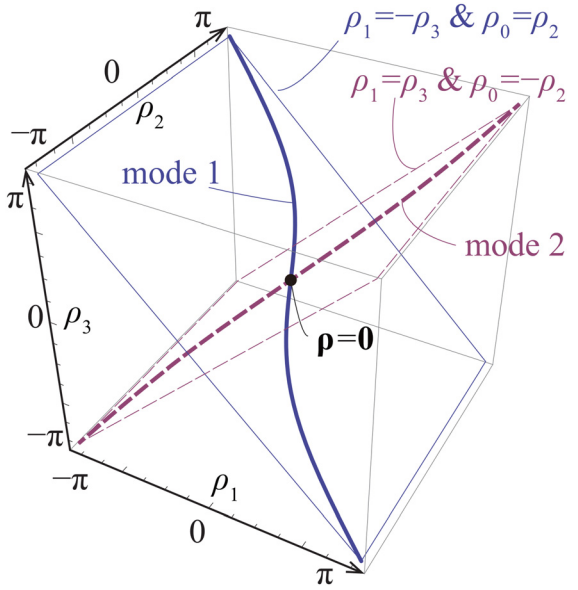

Fig. 4 Visualization of the configuration space of a flat foldable vertex with sector angles $\alpha = \pi/4$ and $\beta = \pi/2$. Note that 4D parameter space is projected along ρ_0 to 3D space formed by ρ_1, ρ_2, and ρ_3. The configuration space is the union of paths of mode 1 and 2. Each path lies on a plane perpendicular to each other.

Therefore, if we start from a point on curve 2 or 1−, the path from the point to $\mathbf{0}$ and through curve 1+ to $\boldsymbol{\rho}_T$ is uniquely self-foldable by U.

Here is a rotational spring potential energy that satisfies conditions 1 and 2

$$U(\boldsymbol{\rho}) = \frac{1}{2}\|\boldsymbol{\rho} - \boldsymbol{\rho}_T\|^2 \tag{7}$$

$$= \sum_{i=0}^{3}\frac{1}{2}(\rho_i - \tau_i)^2 \tag{8}$$

We first prove that $U(\boldsymbol{\rho})$ satisfies condition 1. The energy function on manifold 1 is represented as

$$U_1(\rho_0, -\rho_3, \rho_0, \rho_3) = (\rho_0 - \tau_0)^2 + (\rho_3 - \tau_3)^2 \tag{9}$$

This has a global minimum at the target state. We claim that U_1 has no other local minimum. To see this, rewrite U_1 as a function of single parameter $t = \tan(\rho_o/2)$ in $(-\infty, \infty)$

$$U_1(t) = (2\arctan t - \tau_0)^2 + (2\arctan pt - \tau_3)^2$$

Differentiating U_1 by t, we obtain

$$\frac{dU_1(t)}{dt} = \frac{2}{1+t^2}(\rho_0(t) - \tau_0) + \frac{2p}{1+p^2t^2}(\rho_3(t) - \tau_3)$$

Since $\rho_0(t) - \tau_0$ and $\rho_3(t) - \tau_3$ has the same sign, this takes the value 0 only at the target state.

Next, we prove condition 2. The energy function on manifold 2 is

$$U_2(\rho_0, \rho_3, -\rho_0, \rho_3) = \rho_0^2 + \tau_0^2 + \rho_3^2 + \tau_3^2$$

This has a global minimum only at $\boldsymbol{\rho} = \mathbf{0}$ because

$$\frac{dU_2(t)}{dt} = \frac{2t}{1+t^2} + \frac{2pt}{1+p^2t^2}$$

is zero only at $t = 0$.

Thus, the potential energy given by Eq. (8) uniquely self-folds along a valid rigid folding path from an arbitrary configuration to $\boldsymbol{\rho} = \boldsymbol{\rho}_{\mathbf{T}}$. □

Equation (8) can be simply realized by using rotational springs with rest angles set to target angles; for edge i, we attach a spring with moment $f_i = k(\tau_i - \rho_i)$ (proportional to the angle difference between current and target states). Here, we use the same stiffness $k = 2$ for all of four creases. Also, this is just an example. We may construct a different set of driving forces with different nonlinear springs such that it also satisfies conditions 1 and 2.

5 Unique Self-Foldability From the Flat State

As seen in Theorem 1, the driving force must be carefully designed in order for the self folding to pass through $\boldsymbol{\rho} = \mathbf{0}$ without getting caught on any bifurcations of the configuration space manifold. We can generalize the necessary conditions for unique self-foldability at the flat, unfolded state.

LEMMA 2 (Perpendicular Constraints). *A well-behaved continuous rigid folding $\boldsymbol{\rho}(s)$ from the unfolded state $\boldsymbol{\rho}(0) = \mathbf{0}$ with tangent vector $\boldsymbol{v}_+$ is uniquely self-foldable only if the driving force $\boldsymbol{f}$ at the unfolded state is perpendicular to every tangent vector in the valid tangents not connected to the projection of $\boldsymbol{v}_+$ or $-\boldsymbol{v}_+$ on the unit sphere.*

Proof. Consider the spherical projection of valid tangents at the unfolded state, which is a closed set because the configuration space is a closed set. These projected tangents are arc-wise connected to the projection of the vector $\mathbf{v}_+$ or $-\mathbf{v}_+$. Consider a valid tangent vector $\mathbf{v}_a$ that is not connected to $\mathbf{v}_+$ or $-\mathbf{v}_+$ and assume, for the sake of contradiction, that $\mathbf{v}_a$ is not perpendicular to $\mathbf{f}(0)$, i.e., $\mathbf{v}_a \cdot \mathbf{f}(0) \neq 0$. Because the configuration is in a flat state, flipping all mountains and valleys of the valid folding is also a valid folding by symmetry. Therefore, there are two folding paths with tangent $\pm\mathbf{v}_a$, one of which must make a positive dot product with $\mathbf{f}$, i.e., $f_+ > 0$. Since $\mathbf{v}_a$ is in a closed domain, there is a vector $\mathbf{v}_{\max}$ that is arc-wise connected to $\mathbf{v}_a$ that locally maximizes $\mathbf{v}_{\max} \cdot \mathbf{f}(0)$. Since $\mathbf{v}_{\max}$ is not $\mathbf{v}_+$ or $-\mathbf{v}_+$, there is another self-folding motion, which contradicts the uniqueness of our self folding. □

As a consequence of Lemma 2, we are able to get the following important necessary condition.

LEMMA 3 (Infinitesimal Dimension Constraints). *Consider an origami model at the flat, unfolded state and the tangent $\boldsymbol{v}$ of a desired well-behaved continuous rigid folding. The desired folding is uniquely self-foldable at the flat state only if the dimension m of the solution space of first-order constraints given by Eq. (3) is strictly larger than the number of dimensions n of the linear space spanned by every tangent vector $\boldsymbol{v}_a$ not connected to $\boldsymbol{v}$ or $-\boldsymbol{v}$ via valid tangents.*

Proof. Since the configuration space is tangent to the linear space defined by Eq. (3), we have that $m \geq n$. Assume that $m = n$, then the first-order solution space is exactly the linear space composed of the vectors $\mathbf{v}_a$. Let $\mathbf{v}_1, \ldots \mathbf{v}_n$ be linearly independent vectors spanning this space. Then, $\mathbf{v}$ can be written as a linear combination of these vectors. However, if the model is uniquely self-foldable in the direction of $\mathbf{v}$, then, the force $\mathbf{f}$ must satisfy $\mathbf{v}_i \cdot \mathbf{f} = 0$ for $i = 1, \ldots, n$, which results in $\mathbf{v} \cdot \mathbf{f} = 0$. Therefore, it is not possible to design a driving force $\mathbf{f}$ that self-folds in the direction of $\mathbf{v}$ such that $\mathbf{v} \cdot \mathbf{f} > 0$. □

LEMMA 4 (All Positive Constraints). *A well-behaved rigid folding $\boldsymbol{\rho}(s)$ from the unfolded state $\boldsymbol{\rho}(0) = 0$ with tangent vector $\boldsymbol{v}_+$, when $\boldsymbol{v}_+$ and $-\boldsymbol{v}_+$ are in separate components of valid tangents, is uniquely self-foldable only if the force at the unfolded state forms non-negative dot product, $f_+ \geq 0$, for every tangent vector connected to $\boldsymbol{v}_+$ via valid tangents.*

Proof. Assume that there is a vector $\mathbf{v}_a$ arc-wise connected to $\mathbf{v}_+$ through valid tangent but forms negative dot product: $\mathbf{v}_a \cdot \mathbf{f} < 0$. Then, its opposite vector $-\mathbf{v}_a$, which is connected to $-\mathbf{v}+$ though valid tangents, satisfies $-\mathbf{v}_a \cdot \mathbf{f} > 0$. There is a vector $\mathbf{v}_{\max}$ that is arc-wise connected to $-\mathbf{v}_a$ that locally maximizes $\mathbf{v}_{\max} \cdot \mathbf{f}(0)$. Since $\mathbf{v}_{\max}$ is not $\mathbf{v}_+$, there is another self-folding motion. □

The combination of these necessary conditions are useful to the design of driving forces that make the model uniquely self-fold in a desired way. However, this is not sufficient even locally at the flat state; if the subset of valid tangents that is connected to $\mathbf{v}_+$ forms a wiggly boundary, it will have another local maximum of f_+. In Sec. 6, we use these conditions to prove or disprove unique self-foldability of a rigid origami based on degree-4 vertices.

6 Connecting Degree-4 Flat-Foldable Vertices

In this section, we consider the family of 1DOF rigidly foldable origami generated by connecting vertices of Theorem 1. An obvious example of this is a Miura-ori, but it is not restricted enough for our purposes. A large variety of over-constrained mechanisms can be generated [12–14] by using the linear relationship between opposite fold angles described in tangent of half angle formulas. Such structures also inherit the same nature of the single vertex having separate modes. This makes the structures reconfigurable and reprogrammable into different shapes, but at the same time this makes it difficult for them to self-fold.

LEMMA 5. *If the interior vertices of a well-behaved continuous rigid folding form an $a \times b$ quadrangular grid, then it has exactly $a + b$ linearly independent vectors within the first-order constraints in the flat state.*

Proof. For each interior vertex, the first-order constraint at the flat state is given as

$$\dot{\rho}_0 \boldsymbol{\ell}_0 + \dot{\rho}_1 \boldsymbol{\ell}_1 + \dot{\rho}_2 \boldsymbol{\ell}_2 + \dot{\rho}_3 \boldsymbol{\ell}_3 = \mathbf{0}$$

Consider that edge 0 is at the top and 1 is at the left. For arbitrarily given ρ_0 and ρ_1, there is a solution to ρ_2 (bottom) and ρ_3 (right) satisfying

$$\dot{\rho}_2 \boldsymbol{\ell}_2 + \dot{\rho}_3 \boldsymbol{\ell}_3 = -(\dot{\rho}_0 \boldsymbol{\ell}_0 + \dot{\rho}_1 \boldsymbol{\ell}_1)$$

because $\boldsymbol{\ell}_2$ and $\boldsymbol{\ell}_3$ are not parallel. Consider the global model of a quadrangular grid. If we arbitrarily choose $\dot{\rho}$ for the b edges on the top and the a edges on the left, then this will sequentially determine $\dot{\rho}$ for connecting edges. This leaves an $(a-1) \times (b-1)$ grid with top and left edges assigned with $\dot{\rho}$. This process sequentially determines the infinitesimal folding angle of each edge. □

As the most simple case, consider connecting two flat-foldable vertices as in Fig. 5. In this case, each vertex can choose its mode from 1 to 2 as in Theorem 1, whose combination yields four possible modes.

THEOREM 6. *An origami made of two flat-foldable degree-4 vertices is not uniquely self-foldable from a flat state.*

Proof. There are four possible tangent vectors along four possible modes at the flat unfolded state. Consider that the left vertex has coefficients of p_L, q_L and the right has p_R, q_R. Then, the four infinitesimal modes at flat state can be represented as

$$\begin{bmatrix} 1 & -p_L & 1 & p_L & -p_R & 1 & p_R \\ 1 & \frac{1}{q_L} & -1 & \frac{1}{q_L} & \frac{1}{q_R} & -1 & \frac{1}{q_R} \\ 1 & \frac{1}{q_L} & -1 & \frac{1}{q_L} & -p_R & 1 & p_R \\ 1 & -p_L & 1 & p_L & \frac{1}{q_R} & -1 & \frac{1}{q_R} \end{bmatrix}$$

where each row represents a seven-dimensional infinitesimal mode. The rank of this matrix is 3. Also, the 3×7 subset matrix composed of an arbitrary selection of three rows has rank of 3. Now, assume that one of the modes $\mathbf{v}$ is uniquely self-foldable. Then, the left-over tuple of modes form linearly independent vectors of a three-dimensional space. Because of Lemma 5, we have a $2 + 1 =$ three-dimensional tangent space, and by Lemma 3, $\mathbf{v}$ cannot be a unique self-folding mode. □

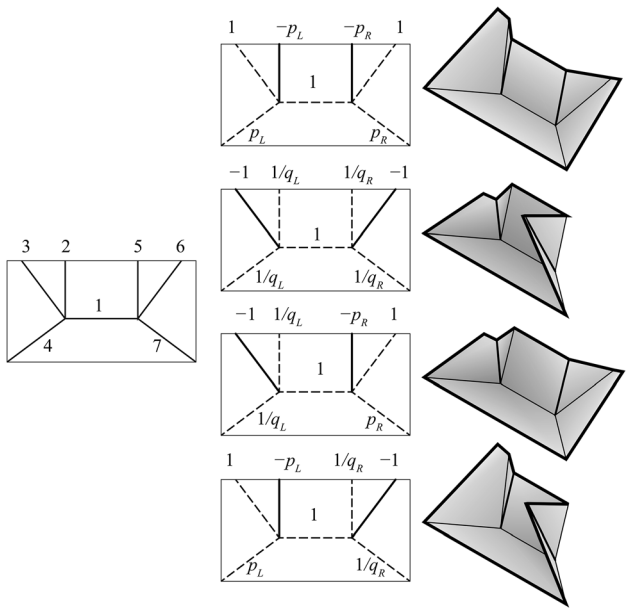

Fig. 5 A model with two flat-foldable vertex having four different folding modes. Left: original crease pattern with edge numbering. Middle: mountain and valley assignments. Right: folded forms.

This means that if there is a self-folding, then, there is always another valid self-folding mode. Comparing the numbers of folding modes and infinitesimal modes provides good insight toward this type of problem.

As another example, consider a regular square twist in Fig. 6 with free mountain-valley assignment. In this structure, all vertices share the same angle $\alpha = (\pi/2)$ and β, and thus, the coefficients are

$$p = p(\alpha, \beta) = q(\alpha, \beta) = \frac{1 - \tan\frac{\beta}{2}}{1 + \tan\frac{\beta}{2}}$$

This does not fold like a conventional square twist (which is not rigidly-foldable), but has distinct six modes as illustrated in the figure. We can obtain these six modes by considering the speed assignments for edges around the center square. Each vertex relates the folding speeds of two adjacent edges. The ratio between the tangent of half the folding angles is either p or $(-1/p)$ depending on the mode chosen for each vertex. Because this forms a closed chain around the square, products of the ratios of four vertices must be 1. As p and $(-1/p)$ can be described as $\sigma\text{sign}(p)\exp(\sigma \log|p|)$ $(\sigma = \pm 1)$, the product of four ratios being 1 is equivalent to obtaining a set of valid signs $\sigma_{i(i+1)}$ $(i = 1,\ldots, 4 \bmod 4)$ that satisfies

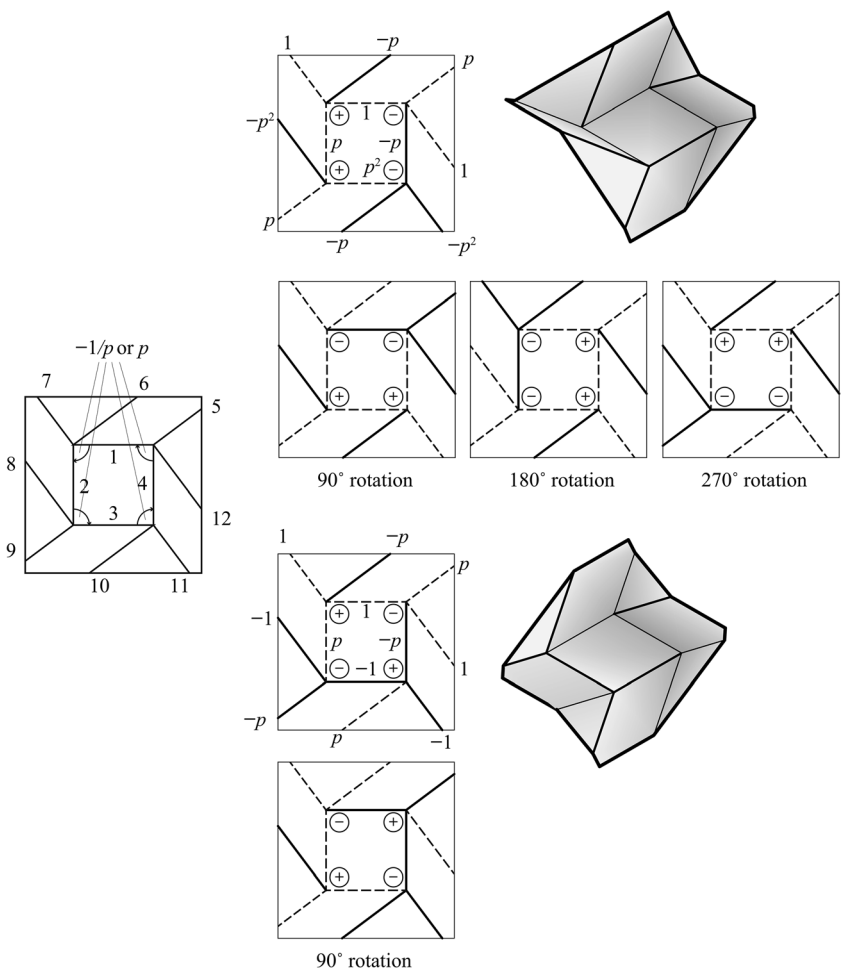

Fig. 6 A regular square twist with six different folding modes. Essentially two modes, one has four rotational variations, and the other has two rotational variations.

$$\sigma_{12}\log|p| + \sigma_{23}\log|p| + \sigma_{34}\log|p| + \sigma_{41}\log|p| = 0$$
$$\sigma_{12}\sigma_{23}\sigma_{34}\sigma_{41} = 1$$

These constraints yield following six variations, which are illustrated in Fig. 6

$$(++--), (-++-), (--++)$$
$$(+--+), (+-+-), (-+-+)$$

THEOREM 7. *A regular square twist model is not uniquely self-foldable from a flat state*.

Proof. According to Lemma 5, the number of dimensions of the tangent space at the flat state is $2+2=4$. The non-normalized tangent vectors along the six modes can be represented as

$$\begin{bmatrix} 1 & p & p^2 & -p & p & -p & 1 & -p^2 & p & -p & -p^2 & 1 \\ p & p^2 & -p & 1 & 1 & -p^2 & p & -p & -p^2 & 1 & p & -p \\ p^2 & -p & 1 & p & p & -p & -p^2 & 1 & p & -p & 1 & -p^2 \\ -p & 1 & p & p^2 & -p^2 & 1 & p & -p & 1 & -p^2 & p & -p \\ 1 & p & -1 & -p & p & -p & 1 & -1 & -p & p & -1 & 1 \\ p & -1 & -p & 1 & 1 & -1 & -p & p & -1 & 1 & p & -p \end{bmatrix}$$

whose rank is 4. Removing row 1 or 5 does not change the rank of the matrix. Because of symmetry, any submatrix composed of five arbitrary rows is also rank 4. According to Lemma 3, this cannot uniquely self-fold from the flat state. □

On the other hand, if the structure has less symmetry, it may uniquely self-fold. Consider a similar twist fold with vertex ratio p and $(-1/p)$ but with one corner having ratio of $-p^3$ and $(1/p^3)$. This will have closure constraints of

$$\sigma_{12}\log|p| + \sigma_{23}\log|p| + \sigma_{34}\log|p| - 3\sigma_{41}\log|p| = 0$$
$$\sigma_{12}\sigma_{23}\sigma_{34}\sigma_{41} = 1$$

This will give only two solutions (σ_{12}, σ_{23}, σ_{34}, and σ_{41}) $=(+++-)$ or $(---+)$, visualized in Fig. 7.

THEOREM 8. The irregular square twist in Fig. 7 is uniquely self-foldable from and to arbitrary states by a rotational spring force.

Proof. The configuration space consists of two modes 1 and 2. Consider a target state $\boldsymbol{\rho}_T = (\tau_1, \ldots, \tau_{12})^{\mathrm{T}}$ in mode 1. Notice that in these two global modes, every vertex also folds in different modes. Here, we construct a potential energy by the summation of potential energy for each vertex, i.e., Eq. (8)

$$U(\boldsymbol{\rho}) = \sum_{i=1}^{4}(\rho_i - \tau_i)^2 + \frac{1}{2}\sum_{i=5}^{12}(\rho_i - \tau_i)^2 \tag{10}$$

In mode 2, the energy function is the summation of functions monotonically decreasing toward the flat-state, which is again monotonically decreasing toward the flat-state. In mode 1, the energy function is the summation of functions monotonically decreasing toward the target state, which is again monotonically decreasing toward the target state. Therefore, the rotational spring energy in Eq. (10) uniquely self-folds to $\boldsymbol{\rho}_T$ from any configuration. □

Equation (10) can be realized by using rotational springs with rest angles set to target angles: for edge i, we attach a spring with moment $f_i = k_i(\tau_i - \rho_i)$ (proportional to the angle difference between current and target states). Here, the stiffness for the creases shared by two interior vertices is $k_i = 4$ $(i = 1\ldots4)$, and the stiffness for the creases shared only by one vertex is $k_i = 2$ $(i = 5\ldots8)$.

One may double-check the perpendicularity at the flat state. Non-normalized tangent vectors along two modes at the flat state can be represented as

$$\mathbf{v}_1 = [1 \;\; p \;\; p^2 \;\; p^3 \;\; -p^3 \;\; -p \;\; 1 \;\; -p^2 \;\; p \;\; -p^3 \;\; p^2 \;\; 1]^{\mathrm{T}}$$
$$\mathbf{v}_2 = [p^3 \;\; -p^2 \;\; p \;\; -1 \;\; -1 \;\; -p^2 \;\; -p^3 \;\; p \;\; p^2 \;\; -1 \;\; -p \;\; -p^3]^{\mathrm{T}}$$

The driving forces toward first and second mode can be represented as

$$\mathbf{f}_1 = [2\tau_1 \;\; 2\tau_2 \;\; 2\tau_3 \;\; 2\tau_4 \;\; -\tau_4 \;\; -\tau_2 \;\; \tau_1 \;\; -\tau_3 \;\; \tau_2 \;\; -\tau_4 \;\; \tau_3 \;\; \tau_1]^{\mathrm{T}}$$
$$\mathbf{f}_2 = [2\tau_1 \;\; 2\tau_2 \;\; 2\tau_3 \;\; 2\tau_4 \;\; \tau_4 \;\; \tau_2 \;\; -\tau_1 \;\; \tau_3 \;\; -\tau_2 \;\; \tau_4 \;\; -\tau_3 \;\; -\tau_1]^{\mathrm{T}}$$

Then, the forces and tangents are perpendicular to each other:

$$\mathbf{f}_1 \cdot \mathbf{v}_2 = \mathbf{f}_2 \cdot \mathbf{v}_1 = 0$$

7 Degree-6 Vertex

Finally, we come back to the degree-6 vertex shown in Fig. 1. As already mentioned, the driving force toward the correct mountain and valley assignment, $\mathbf{f} = (f, -g, f, -g, f, -g)^{\mathrm{T}}$ $(f, g > 0)$, at the flat state can self-fold into either of pop-up or pop-down states since both of them share the same mountain-valley assignment, and thus, this driving force will not uniquely self-fold. We will show an insight toward designing the same vertex to uniquely self-fold into one of the states in Fig. 1.

This vertex with six creases has three degrees-of-freedom in a generic state. For simplicity, we assume threefold symmetry and treat it as a 1DOF mechanism. As this is a more restrictive configuration space, unique self-folding in this set-up does not imply actual self-folding; we will discuss the generalization later.

7.1 Configuration With Threefold Symmetry. Assume that the configuration can be represented as $\boldsymbol{\rho} = [\rho_A, \rho_B, \rho_A, \rho_B, \rho_A, \rho_B]^{\mathrm{T}}$. Then, the closure constraint (1) can be transformed into the following form:

$$\{\mathbf{R}_x(\rho_A)\mathbf{R}_z(60\,\mathrm{deg})\mathbf{R}_x(\rho_B)\mathbf{R}_z(60\,\mathrm{deg})\}^3 = \mathbf{I}_3 \tag{11}$$

where $\mathbf{R}_x(\rho)$ is rotation about x axis by ρ and $\mathbf{R}_z(\theta)$ is rotation about z axis by θ, which can be written as

$$\mathbf{R}_x(\rho) = \begin{bmatrix} 1 & 0 & 0 \\ 0 & \cos\rho & -\sin\rho \\ 0 & \sin\rho & \cos\rho \end{bmatrix}$$
$$\mathbf{R}_z(\theta) = \begin{bmatrix} \cos\theta & -\sin\theta & 0 \\ \sin\theta & \cos\theta & 0 \\ 0 & 0 & 1 \end{bmatrix}$$

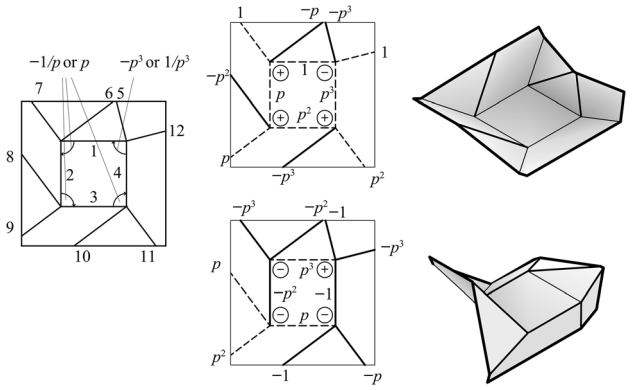

Fig. 7 An irregular "twist" with two different folding modes. Here, $p = 1/2$ in the crease pattern.

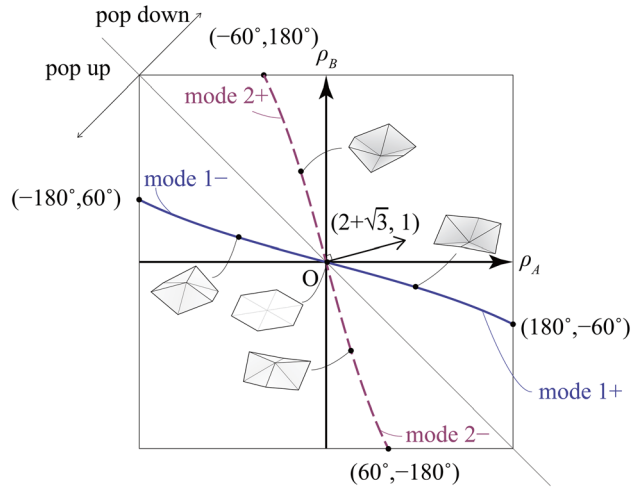

Fig. 8 The configuration space of a degree-6 vertex with threefold symmetry described by solid and dashed curves. At the flat state, the force along $(2+\sqrt{3}, 1)$ should be chosen to uniquely fold toward mode 1+.

Equation (11) is equivalent to saying that $\mathbf{R}_{1/3} := \mathbf{R}_x(\rho_A)\mathbf{R}_z(60\,\text{deg})\mathbf{R}_x(\rho_B)\mathbf{R}_z(60\,\text{deg})$ is a $\phi = 120\,\text{deg}$ rotation about some axis.[1] According to Rodrigues' Formula, the rotation angle ϕ and the trace of the rotation matrix has the following relation:

$$\text{Trace}\left(\mathbf{R}_{1/3}\right) = 2\cos\phi + 1 = 0$$

which is calculated as

$$\text{Trace}\left(\mathbf{R}_{1/3}\right) = \frac{5}{4}\cos\rho_A\cos\rho_B - \sin\rho_A\sin\rho_B - \frac{3}{4}(\cos\rho_A + \cos\rho_B) + \frac{1}{4}$$

Then, we obtain

$$\left(3\cos\frac{\rho_A+\rho_B}{2} - \cos\frac{\rho_A-\rho_B}{2} + 2\right) \times \left(3\cos\frac{\rho_A+\rho_B}{2} - \cos\frac{\rho_A-\rho_B}{2} - 2\right) = 0 \tag{12}$$

In order for the configuration to have no self-intersections, the measure of the solid angle formed by the vertex calculated as $2\pi - 3(\rho_A + \rho_B)$ must exist in $[0, 4\pi]$. Therefore

$$\frac{1}{2} \le \cos\frac{\rho_A+\rho_B}{2} \le 1$$

Equation (12) is satisfied if and only if

$$3\cos\frac{\rho_A+\rho_B}{2} - \cos\frac{\rho_A-\rho_B}{2} - 2 = 0 \tag{13}$$

This forms a configuration space composed of two curves intersecting at the flat state (Fig. 8). The folding path can be simplified as follows:

$$\begin{bmatrix}\tan\frac{\rho_A}{4}\\ \tan\frac{\rho_B}{4}\end{bmatrix} = \begin{cases}\begin{bmatrix}(2+\sqrt{3})t\\ -t\end{bmatrix} & \text{mode 1}\\ \begin{bmatrix}-t\\ (2+\sqrt{3})t\end{bmatrix} & \text{mode 2}\end{cases} \tag{14}$$

[1] $\phi = 0$ yields solution of flat-folding $\rho_A = \pm\pi$ and $\rho_B = \mp\pi$, but does not lead to a valid folding because there is no layer ordering.

This folding motion has the following velocity in the flat, unfolded state

$$\mathbf{v}_1|_{\boldsymbol{\rho}=\mathbf{0}} = \begin{bmatrix}2+\sqrt{3}\\ -1\end{bmatrix} \tag{15}$$

$$\mathbf{v}_2|_{\boldsymbol{\rho}=\mathbf{0}} = \begin{bmatrix}-1\\ 2+\sqrt{3}\end{bmatrix} \tag{16}$$

This tells us that in order to uniquely self-fold to the pop-down state in mode 1 from the flat state, we must choose a force that is perpendicular to $\mathbf{v}_2|_{\boldsymbol{\rho}=\mathbf{0}}$ by Lemma 2. This means that we should use a force parallel to

$$\begin{bmatrix}2+\sqrt{3}\\ 1\end{bmatrix}$$

at the flat state. Thus, a set of weak valley and stronger (approximately 3.73 times stronger) valley force assignments is necessary, instead of a native assignment following that of the target shape (alternating mountains and valleys). In fact, in the symmetric case a proper driving force uniquely self-folds the vertex.

THEOREM 9. *The regular degree-6 vertex with threefold symmetry constraints is uniquely self-foldable from and to arbitrary states by a rotational spring force.*

Proof. Consider that the target state $\boldsymbol{\rho}_T = [\tau_A\,\tau_B]^{\text{T}}$ is in mode 1, and exists in $\tau_A \ge 0$. We may reparameterize:

$$\begin{bmatrix}\tan\frac{\tau_A}{4}\\ \tan\frac{\tau_B}{4}\end{bmatrix} = \begin{bmatrix}(2+\sqrt{3})t_T\\ -t_T\end{bmatrix}$$

Thus, if we use the tangent of quarter angle as the axes for the parameter space, the configuration space is represented by straight lines (Fig. 9). As the derivative of $\tan(\rho/4)$ with respect to ρ is positive in $-180\,\text{deg} < \rho < 180\,\text{deg}$, the signs of the forward force along a folding path are preserved in this remapped parameter space.

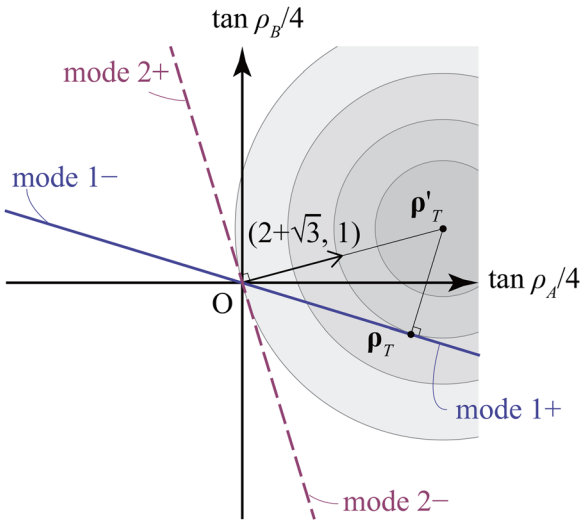

Fig. 9 The configuration space remapped using the tangents of quarter angles. $\boldsymbol{\rho}_T$ is the actual target that we desire, from which off-configuration target $\boldsymbol{\rho}'_T$ is derived. A rotational spring potential energy toward $\boldsymbol{\rho}'_T$ (Eq. (17)), illustrated by gray area, will uniquely drive from any point on the configuration space to $\boldsymbol{\rho}_T$ along the configuration space. Note that there is no bifurcation at (0, 0) because energy increases in both modes 2+ and 2−.

Therefore, our objective is to construct a potential energy that strictly minimizes toward $\boldsymbol{\rho}_T$ along mode 1 and strictly minimizes to $\boldsymbol{\rho} = \mathbf{0}$. We may construct such a rotational spring energy by considering an off-configuration target $\boldsymbol{\rho}'_T = (\tau'_A, \tau'_B)$, which is, in the remapped parameter space, the intersection point of the ray passing through origin toward the direction of $[2+\sqrt{3}, 1]^{\mathrm{T}}$ and the line passing through $\boldsymbol{\rho}_T$ perpendicular to the tangent $\mathbf{v}_1$ at $\boldsymbol{\rho}_T$. Such a point always exists because the folding path exists on a straight line.

We construct the spring potential energy which minimizes at $\boldsymbol{\rho}'_T$

$$U = \frac{1}{2}\left(\tan\frac{\rho_A}{4} - \tan\frac{\tau'_A}{4}\right)^2 + \frac{1}{2}\left(\tan\frac{\rho_B}{4} - \tan\frac{\tau'_B}{4}\right)^2 \tag{17}$$

This energy is quadratic in this remapped parameter space, and strictly minimizes to $\boldsymbol{\rho} = \mathbf{0}$ along mode 2 and strictly minimizes to $\boldsymbol{\rho}_T$ along mode 1, and thus, energy (17) uniquely self-folds under a threefold symmetry constraint. □

7.2 Validity Without Symmetry Constraints. We conjecture that this symmetric path is actually a valid self-folding path even without the symmetry constraint. This can be verified by considering the orthogonal projection $\mathbf{f}_{\mathrm{proj}}$ of the driving force $\mathbf{f}$ to the solution space of first-order constraints. Figure 10 illustrates the crease lines in the folded position. Applying the spherical laws of sines, we obtain that the vector position of the creases $\mathbf{L}_i$ $(i = 0,\ldots,5)$ in mode 1 can be represented as

$$\mathbf{L}_i = \begin{cases} \left[\cos\dfrac{-\rho_B}{2}\cos\dfrac{\pi}{3}i, \quad \cos\dfrac{-\rho_B}{2}, \quad \sin\dfrac{-\rho_B}{2}\right]^{\top} & i\text{: even} \\ \left[\cos\dfrac{-\rho_A}{2}, \quad \cos\dfrac{-\rho_A}{2}, \quad \sin\dfrac{-\rho_B}{2}\right]^{\top} & i\text{: odd} \end{cases}$$

The first-order constraint is given using the 3×6 matrix $\mathbf{C} = [\mathbf{L}_0,\ldots,\mathbf{L}_5]$ as

$$\mathbf{C}\dot{\boldsymbol{\rho}} = \mathbf{0}$$

The orthogonal projection matrix to the first-order solution space is given by

$$\mathbf{P} = [\mathbf{I}_6 - \mathbf{C}^{\mathrm{T}}(\mathbf{C}\mathbf{C}^{\mathrm{T}})^{-1}\mathbf{C}]$$

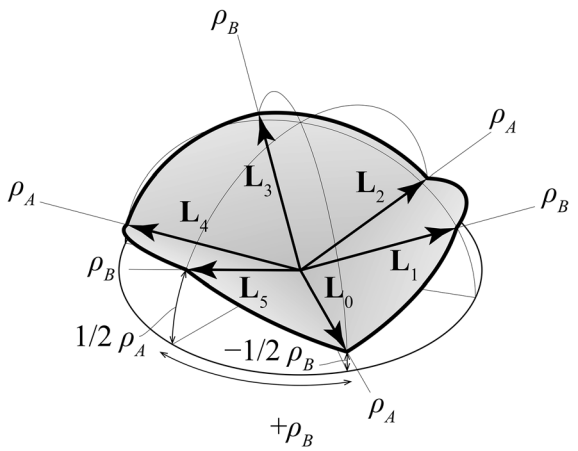

Fig. 10 Crease line position in the folded state

We can now observe from a numerical plot that

$$\mathbf{P}\begin{bmatrix}\mathbf{f}_{1A}\\ \mathbf{f}_{1B}\\ \mathbf{f}_{1A}\\ \mathbf{f}_{1B}\\ \mathbf{f}_{1A}\\ \mathbf{f}_{1B}\end{bmatrix} = c\begin{bmatrix}v_A\\ v_B\\ v_A\\ v_B\\ v_A\\ v_B\end{bmatrix}$$

for some $c > 0$, i.e., the projected driving force is parallel to the symmetric folding mode 1 for any $0 \le t \le 0.5$ and $0 \le t_T \le 0.5$. This means that the constrained force $\mathbf{v}\cdot\mathbf{f}_1$ is maximized in the direction of $\mathbf{v} = \mathbf{v}_1$, so there is a symmetric self-folding motion along mode 1. Although we did not check if constrained force along $\mathbf{v}_1$ is the only local maximum, we believe this is so. If it is, the rotational spring force can uniquely self-fold a degree-6 vertex.

8 Conclusion

In this paper, we proposed a mathematical model of self-folding, specifically for unique-self folding by rotational spring driving forces. We provided necessary conditions for self-foldability that serve as tools to analyze and design self-foldable crease patterns. Using these tools, we demonstrated several results: a degree-4 flat-foldable vertex is uniquely self-foldable; two-vertex and regular twist models based on these vertices are not uniquely self-foldable, but we can design a nonregular twist, that is, uniquely self-foldable. Also, we demonstrated the self-foldability of a degree-6 vertex using the driving force with alternating strong and weak valleys. We believe that these tools can be a basis for future design methods of mechanisms and robotics based on origami. In particular, each of the examples with self-foldability forms a configuration space branching out to different 1DOF mechanisms, while we can assign driving forces that correctly make it choose one of the target modes. This controllability leads to the design of reprogrammable origami systems that can fold into different mechanisms. However, the characterization of self-foldability is still an open problem, and we would like to explore further in this direction.

Acknowledgment

The first author was supported by the JST PRESTO program and JSPS KAKENHI 16H06106. The second author was supported by NSF grant EFRI ODISSEI 1240441.

Nomenclature

Parameters in Crease Patterns and Folded States

- e_{in} = number of creases in a crease pattern
- ℓ_i = normalized direction vector of edge i from the vertex in a flat unfolded state
- $\mathbf{L}_i$ = normalized direction vector of edge i from the vertex in a folded state
- p, q = coefficients of a degree-4 flat-foldable origami vertex
- ρ_i = fold angle, i.e., the supplementary angle of dihedral angle at the fold line i
- v_{in} = number of interior vertices in a crease pattern
- τ_i = target fold angle of fold line i

Variables in the Parameter Space

- $\mathbf{f}(\boldsymbol{\rho})$ = driving force (a set of applied moments). Vector
- $f(s)$ = constrained force along $\mathbf{v}$, defined by $\mathbf{f}(\boldsymbol{\rho}(s)) \cdot \mathbf{v}(s)$
- s = an arclength parameter of a folding path
- t = a parameter of a folding path
- $\mathbf{t}$ = a vector representing the current configuration by tangents of half fold angles. i-th element is $\tan\frac{1}{2}\rho_i$

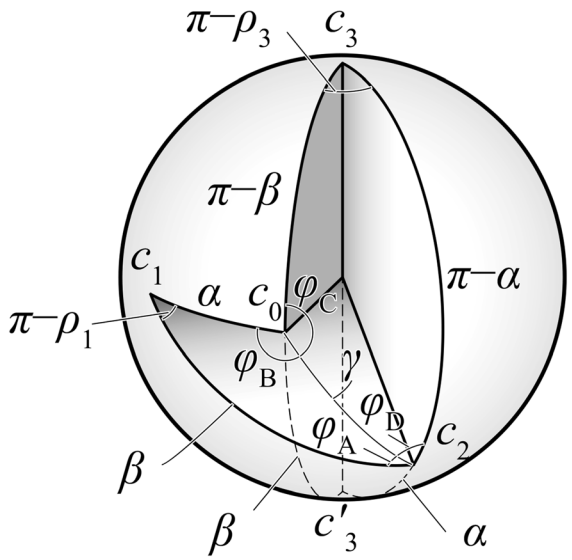

Fig. 11 Napier's analogies

$U(\boldsymbol{\rho})$ = potential energy of the applied moments. Scalar.
$\mathbf{v}(s)$ = normalized tangent vector of a folding path in parameter space
$\boldsymbol{\rho}$ = a vector representing the current configuration. i-th element is ρ_i
$\boldsymbol{\rho}(s)$ = a folding path
$\boldsymbol{\rho}_T$ = configuration of the target position. i-th element is τ_i, the target folding angle of fold line i

Appendix: Proof of Eq. (4)

THEOREM 10. *The configuration space of a degree-4 flat-foldable vertex is the union of Eq. (4).*

Proof. For necessity, consider that there exists a folded state, and consider a spherical intersection of the vertex with a unit sphere. This is a four-bar spherical linkage with edge lengths of sector angles.

Now, we can check the symmetry of Eq. (4) by replacing α by $\pi-\alpha$ or α by β. This means that we can safely assume that α is (one of) the smallest angle(s) of four sector angles.

Also, because the configuration space is symmetric with respect to $\boldsymbol{\rho}=\mathbf{0}$, assume that this vertex is popped down as the pop-up state can always expressed by negating all fold angles of pop-down state. From single-vertex rigid foldability [4], the vertex must have three valley creases c_a, c_b, c_c forming sector angles strictly less than π, and 1 mountain crease c_d.

Now, the pop-down state is possible if and only if

(1) $\alpha<\pi-\beta$ and the assignment of c_0, c_1, c_2, c_3 is V, M, V, V.
(2) $\alpha=\pi-\beta$ and the assignment of c_0, c_1, c_2, c_3 is $V, 0, V, 0$.
(3) $\alpha<\beta$ and the assignment of c_0, c_1, c_2, c_3 is M, V, V, V.
(4) $\alpha=\beta$ and the assignment of c_0, c_1, c_2, c_3 is $0, V, 0, V$.

where M, V, 0 refer to mountain, valley, and uncreased, respectively. The folding of case 2 satisfies mode 1 with $p_a=0$. Similarly, the folding of case 4 satisfies mode 2 with $p_b=0$.

In case 3, the vertex is expressed as a quadrangle on the sphere whose interior is the front side of the vertex. The quadrangle is convex at c_1, c_2, c_3, and concave at crease c_0, so the geodesic segment between c_0 and c_2 lies inside this quadrangle (Fig. 11). Therefore, segment c_0c_2 divides the quadrangle into two triangle composed of convex angles. Let $\gamma<\pi$ denote the length of c_0c_2. Now, we consider the opposite point c_3' of c_3. Then, the angle $\angle c_0c_3'c_2$ equals $\pi-\rho_3$ because $c_3c_3'=\pi$. Now, triangle $c_0c_1c_2$ and $c_0c_3'c_2$ are congruent to each other both of them share segment lengths α, β, $\gamma<\pi$. Because these triangle share the same base angles, $\phi_B=\pi-\phi_D$ and $\phi_C=\pi-\phi_A$. Then, we get that $\rho_0=\phi_B+\phi_C-\pi=\pi-\phi_A-\phi_D=\rho_2$.

Now, use Napier's Analogies of spherical trigonometry to get the following relations:

$$\frac{\tan\frac{\rho_2}{2}}{\tan\frac{\rho_1}{2}}=\frac{\tan\frac{\phi_B-\phi_A}{2}}{\cot\frac{\pi-\rho_1}{2}}=-\frac{\sin\frac{\alpha-\beta}{2}}{\sin\frac{\alpha+\beta}{2}}=-\frac{\tan\frac{\alpha}{2}-\tan\frac{\beta}{2}}{\tan\frac{\alpha}{2}+\tan\frac{\beta}{2}}$$

Such a folding can be represented by the mode 2 of Eq. (4). Similarly, the folding of case 1 satisfies mode 1 of Eq. (4).

For sufficiency, Eq. (4) satisfies Eq. (1). Therefore, Eq. (4) represents the entire configuration space of the vertex.

References

[1] Hawkes, E., An, B., Benbernou, N. M., Tanaka, H., Kim, S., Demaine, E. D., Rus, D., and Wood, R. J., 2010, "Programmable Matter by Folding," Proc. Natl. Acad. Sci. U. S. A., **107**(28), pp. 12441–12445.
[2] Felton, S., Tolley, M., Demaine, E., Rus, D., and Wood, R., 2014, "A Method for Building Self-Folding Machines," Science, **345**(6197), pp. 644–646.
[3] Na, J.-H., Evans, A. A., Bae, J., Chiappelli, M. C., Santangelo, C. D., Lang, R. J., Hull, T. C., and Hayward, R. C., 2015, "Programming Reversibly Self-Folding Origami With Micropatterned Photo-Crosslinkable Polymer Trilayers," Adv. Mater., **27**(1), pp. 79–85.
[4] Abel, Z., Cantarella, J., Demaine, E. D., Eppstein, D., Hull, T. C., Ku, J. S., Lang, R. J., and Tachi, T., 2016, "Rigid Origami Vertices: Conditions and Forcing Sets," J. Comput. Geom., **7**(1), pp. 171–184.
[5] Akitaya, H., Cheung, K., Demaine, E. D., Horiyama, T., Hull, T. C., Ku, J., and Tachi, T., 2016, "Rigid Foldability With Optional Creases is NP-Hard," (Unpublished).
[6] Hanna, B. H., Magleby, S. P., Lang, R. J., and Howell, L. L., 2015, "Force-Deflection Modeling for Generalized Origami Waterbomb-Base Mechanisms," ASME J. Appl. Mech., **82**(8), p. 081001.
[7] Waitukaitis, S., Menaut, R., Chen, B. G., and van Hecke, M., 2015, "Origami Multistability: From Single Vertices to Metasheets," Phys. Rev. Lett., **114**(5), p. 055503.
[8] Silverberg, J. L., Evans, A. A., McLeod, L., Hayward, R. C., Hull, T., Santangelo, C. D., and Cohen, I., 2014, "Using Origami Design Principles to Fold Reprogrammable Mechanical Metamaterials," Science, **345**(6197), pp. 647–650.
[9] Kawasaki, T., 1997, "$R(\gamma)=\mathbf{I}$," Second International Meeting of Origami Science and Scientific Origami, pp. 31–40.
[10] Belcastro, S., and Hull, T., 2002, "A Mathematical Model for Non-Flat Origami," Origami^3: 3rd International Meeting of Origami Mathematics, Science, and Education, pp. 39–51.
[11] Tachi, T., 2016, "Rigid Folding of Periodic Triangulated Origami Tessellations," Origami^6: Sixth International Meeting on Origami Science, Mathematics, and Education, K. Miura, T. Kawasaki, T. Tachi, R. Uehara, P. Wang-Iverson, and R. J. Lang, eds., pp. 97–108.
[12] Tachi, T., 2010, "Freeform Rigid-Foldable Structure Using Bidirectionally Flat-Foldable Planar Quadrilateral Mesh," Advances Architectural Geometry 2010, Springer, Vienna, Austria, pp. 87–102.
[13] Tachi, T., 2009, "Generalization of Rigid-Foldable Quadrilateral-Mesh Origami," J. Int. Assoc. Shell Spatial Struct., **50**(3), pp. 173–179.
[14] Evans, T. A., Lang, R. J., Magleby, S. P., and Howell, L. L., 2016, "Rigidly Foldable Origami Twists," Origami^6: Sixth International Meeting on Origami Science, Mathematicsw, and Education, K. Miura, T. Kawasaki, T. Tachi, R. Uehara, P. Wang-Iverson, and R. J. Lang, eds., pp. 119–130.